Analytical Methods

ROYAL SOCIETY OF CHEMISTRY

PAPER

View Article Online
View Journal | View Issue

Cite this: *Anal. Methods*, 2020, **12**, 5833

An electroosmotic flow-free two-direction migration strategy enables fast affinity capillary electrophoresis to study the weak interactions between basic peptides and RNA†

Zheng Yuan, [ab] Peng Xu, [c] Fangzhi Yu, [ab] Dapeng Zhang, [ab] Qiang Zhao,[ab] Wenqiang Yu[c] and Hailin Wang *[abd]

Received 8th August 2020
Accepted 6th November 2020

DOI: 10.1039/d0ay01515f

rsc.li/methods

Affinity Capillary Electrophoresis (ACE) is a useful analytical tool to study noncovalent interactions. However, it remains challenging for ACE to measure weak and unstable interactions due to the fast dissociation of the binding complex and the possible destruction of the complex by a high electric field. In this study, we proposed a two-direction migration strategy that enables ACE to detect weak and unstable but important interactions by decreasing the migration distance of the binding complex and controlling the opposite migration direction of the free probe. By synthesizing a polyacrylamide-coated neutral capillary, free of electroosmotic flow, two-direction CE migration of basic peptides (positively charged) and peptide–RNA complexes (negatively charged) was achieved. Furthermore, the weak interactions between small nuclear U2 RNA and histone peptides were detected by this two-direction migration CE approach. The effects of the methylation states of histone peptides on the weak peptide–RNA interactions were also explored by this new approach. Collectively, the suggested modification of the ACE method is able to qualitatively characterize weak interactions.

1. Introduction

Affinity Capillary Electrophoresis (ACE) is a useful method based on the measurements of the migration velocity to study affinity interactions.[1–3] ACE shares the same advantages as CE, including high resolution, short time consumption, and low reagent consumption.[4] Besides, relying on detectors, such as laser-induced fluorescence (LIF)[5,6] and mass spectrometry (MS),[7] ACE is able to sensitively analyse the interactions of protein–protein,[8–12] peptide complexes,[13] protein–DNA/RNA6,[14–17] protein-small molecules,[18–21] and DNA-small molecules.[22] Particularly, when ACE is coupled with highly sensitive LIF detection, many new biological phenomena and molecular mechanisms in the field of DNA damage and repair,[15,23–26] epigenetics,[17] and host–virus interactions[27,28] have been discovered. Widening the application of ACE in biology may promote gaining information on and insights into biological mechanisms, genetic and epigenetic diseases, and even viral infection.[28]

It is notable that many noncovalent interactions are weak, dynamic and transient. Despite these features, weak interactions are also important to maintain physiological functions. It remains challenging for ACE to measure these unstable interactions because binding complexes may easily dissociate and/or even be destroyed by the strong electric field during CE separation.[29] We reported that adding serum albumin or IgG in sample buffer can reduce nonspecific adsorption and enhance the stability of the protein–DNA complexes during CE separation.[30,31] Ouimet *et al.* developed a PXCE (protein cross-linking capillary electrophoresis) method which is able to maintain noncovalent binding by adding cross-linking reagents to equilibrated samples prior to CE separation.[32] In this study, we propose an electroosmotic flow-free two-direction migration strategy for affinity CE to measure these weak and unstable interactions.

Binding parameters of affinity interactions can be estimated from the dissociation trace of the pre-equilibrated complex during CE separation.[33] Nevertheless, when binding is too weak or dissociation is too fast, the dissociation trace cannot be detected. To address this issue, one probable strategy is to shorten the separation time to decrease undesired dissociation

[a]*The State Key Laboratory of Environmental Chemistry and Ecotoxicology, Research Center for Eco-Environmental Sciences, Chinese Academy of Sciences, Beijing 100085, China. E-mail: hlwang@rcees.ac.cn; Tel: +86-10-6284 9600*

[b]*University of Chinese Academy of Sciences, Beijing 100049, China*

[c]*Shanghai Public Health Clinical Center and Department of General Surgery, Huashan Hospital, Cancer Metastasis Institute and Laboratory of RNA Epigenetics, Institutes of Biomedical Sciences, Shanghai Medical College, Fudan University, Shanghai, 201508, China*

[d]*University of Jianghan, Wuhan, Hubei 430056, China*

† Electronic supplementary information (ESI) available. See DOI: 10.1039/d0ay01515f

during electrophoresis. However, short migration usually conflicts with resolution required for traditional ACE to distinguish the binding complex from the free probe. Herein, to solve this contradiction, we propose a two-direction migration strategy by which the pre-equilibrated sample mixture is loaded near the detection window under the binding conditions to allow rapid identification of the unstable complex from the free probe which is adjusted to migrate to the opposite direction (Fig. 1). The utility of this strategy was tested by investigating the weak interactions between small nuclear (sn) RNA U2 and two basic peptides derived from human histone H3 and H4. The effects of the methylation states of peptides on their binding were also explored by this approach. Notably, the inner wall of the capillary used was coated with polyacrylamide (PAA) to eliminate the electroosmotic flow (EOF),[34,35] achieving two-direction migration of basic peptide probes and negatively charged peptide–RNA complexes. Simultaneously, the adsorption of positively charged basic peptides was overcome by PAA modification.

2. Experimental section

2.1 Chemicals and reagents

All reagents including methanol, acetone, and acetic acid were of analytical reagent (AR) grade and purchased from the National Pharmaceutical Group Chemical Reagent Company (Beijing, China); glycine and tris-(hydroxymethyl)aminomethane (Tris) were of biotechnology grade and supplied by Ameresco (Tully, NY, USA). γ-Mercaptopropyl trimethoxysilane (γ-MPS, 97%) was provided by Macklin Biochemical Co. Ltd. (Shanghai, China). Acrylamide (AR) was purchased from Aladdin (Beijing, China). *N*,*N*,*N*,*N*-tetramethylethylenediamine (TEMED, ≥ 99%) and ammonium persulfate (APS, 98%) were purchased from Sigma-Aldrich (St. Louis, MO, USA) and Sangon Biotech Co., Ltd. (Shanghai, China), respectively. The fluorescein isothiocyanate isomer I (FITC, ≥ 90%) was purchased from Solarbio Science and Technology Co., Ltd. (Beijing, China). Sodium hydroxide (GR), hydrochloric acid (GR), and sodium chloride (GR) were all supplied by Beijing Chemical Factory (Beijing, China). The ribonuclease A (RNase A) was purchased from Worthington Biochemical (NJ, USA). All solutions were prepared using ultrapure water from a Purelab Ultra Elga Lab-water system (VWS Ltd., UK) with an electrical resistivity of 18.2 MΩ cm and filtered through a 0.45 μm filter.

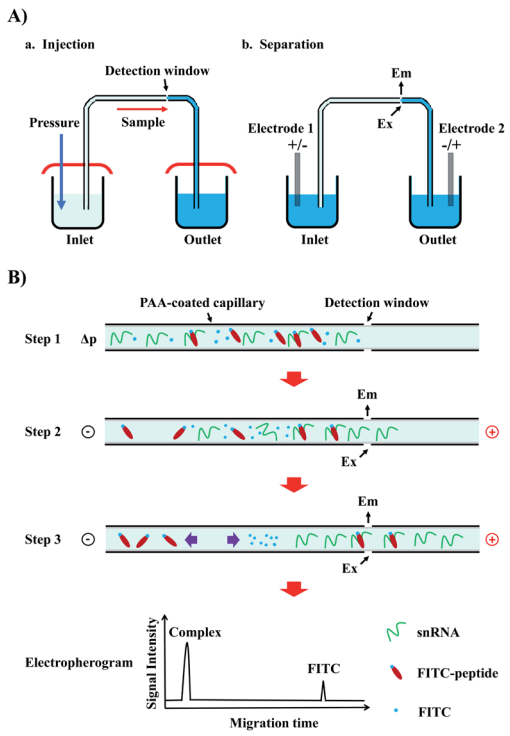

Fig. 1 Schematic illustration of the analytical principle of the EOF-free two-direction migration strategy to monitor weak peptide–RNA interactions. (A) Scheme of sample injection (left) and separation (right). (B) Scheme of two-direction CE migration (purple arrows in step 3) of the substrates of interest and the predicted electropherograms.

2.2 Oligonucleotides and snRNA

A pair of complementary oligonucleotide probes used in the experiment were synthesized and purified by Sangon. DNA hybridization and purification experiments were as previously described.[36,37]

The sequence is: 5′-TTATCGTGTAAGTAACCCGCCTACTG-GATATTGTCCCCAGCATTTAAAACCTCTGCCGTAAGC-GATGTCCTGGCCCCTCCTCAGCACCTTATC-3′.

The U2 snRNA was synthesized as described previously.[38]

2.3 Peptides

The peptides were synthesized and purified by GenScript (Nanjing, China). The sequences are as follows (N′–C′):

H3K9 peptide: FITC–ARTKQTARKSTGGKAPRKQLA

H3K9me2 peptide: FITC–ARTKQTARK^{me2}STGGKAPRKQLA

H4R3 peptide: FITC–SGRGKGGKGLGKGGAKRHRKV

H4R3me peptide: FITC–SGR^{me}GKGGKGLGKGGAKRHRKV-

where FITC represents the labelled fluorophore at the N-terminus; K^{me2} and R^{me} represent dimethylated lysine and monomethylated arginine, respectively.

2.4 Equipment

The oven for temperature controlling was purchased from Sopu instrument (Shanghai, China). A K30 dry bath incubator was supplied by Allsheng instrument Co. Ltd. (Hangzhou, China) and was used to control the temperature of peptide–DNA/RNA reactions. ACE-LIF analysis was performed on a P/ACE MDQ system (Beckman Coulter, CA, USA) coupled with a LIF detector with an excitation wavelength of 488 nm and an emission wavelength of 520 nm. An uncoated fused-silica capillary with an inner diameter of 50 μm and an outer diameter of 375 μm was purchased from Yongnian Technologies (Hebei, China). The total length of the capillary was 31 cm, and the effective length was 21 cm.

2.5 FITC–DNA and peptide–RNA incubation

For testing a suspected FITC–DNA interaction, 20.0 nM 93-bp double-stranded DNA (dsDNA) was incubated with different concentrations of FITC (2.0 pM–2.0 nM as indicated) in 1.0 × TH buffer (50 mM Tris–HCl, pH 7.4) at 37 °C for 10.0 min. For measuring peptide–RNA interactions, each peptide (40 M) was mixed with different concentrations of snRNA U2 in 1.0 × TH buffer supplemented with 50.0 mM NaCl, and incubated at 37 °C for 30 min.

2.6 PAA modification of the capillary

First, a 50.0 cm long fused-silica capillary was cut off and flushed with methanol for 30.0 min, water for 5.0 min, acetone for 30.0 min, and water for 5.0 min, to remove the possible stains on the inner wall. The capillary was then infused and etched with 1.0 M NaOH for 1.0 h to expose negatively charged silicon–oxygen bonds and then flushed with water for 5.0 min, 1.0 M HCl for 1.0 h, and finally water for 5.0 min. Secondly, the capillary was coated with γ-MPS, a linker for acrylamide. 100 μL of γ-MPS was mixed with 1.0 mL of methanol solution which was prepared by dissolving 100 μL of methanol in 900 μL of ultrapure water and adjusted to pH 3.5 by acetic acid. The prepared γ-MPS solution was then infused into the capillary. After blocking the two ports with silicone plugs, the capillary was placed in an oven at 37.0 °C for 90.0 min. Notably, two more rounds of γ-MPS modification were conducted to ensure a complete γ-MPS coating. After flushing with water for 10.0 min, the capillary was purged with nitrogen for over 8.0 h at 80 °C to remove water adhering to the inner wall and to ensure good γ-MPS immobilization. Third, the γ-MPS-modified capillary was reacted with acrylamide. For this purpose, PAA solution was freshly prepared by quickly mixing 10.0 μL of TEMED (10.0% v/v) and 10.0 μL of APS (10.0% m/v) with 1.0 mL of acrylamide solution (4.0% m/v) and was immediately infused into the γ-MPS-modified capillary. Notably, prior to PAA solution preparation, the acrylamide solution was flushed with nitrogen for 30.0 min to remove dissolved oxygen. After 1 min injection of PAA solution, the capillary was quickly sealed at both ends with silicone plugs. After 2.0 h-incubation at room temperature, the capillary was flushed with water for 10.0 min and purged with nitrogen at 80 °C for 2.0 h. The PAA-coated capillary was sealed by silicone plugs and kept in a glass vacuum dryer. The capillary was flushed and equilibrated with 2 × TGA buffer (14.0 mM Tris, 108.0 mM glycine, 10.5 mM HAc, pH 7.5) for 20.0 min prior to use.

2.7 CE analysis

The pre-equilibrated reaction mixture was injected at a pressure of 6.9×10^4 pascal (pa) for 8.0 s. The injected volume was optimized to make the loaded sample approach the detection window. The mixture was then separated in 2.0 × TGA buffer with a voltage of −15.0 kV for 8.0 min. A laser of 488 nm was used to excite FITC. Before each run, the capillary was flushed using 2.0 × TGA buffer at a negative voltage −20.0 kV and 3.45×10^4 pa for 2.0 min.

3. Results and discussion

3.1 Principle of two-direction migration affinity CE analysis

We first coupled a P/ACE MDQ system (Beckman Coulter, CA, USA) with a LIF detector which allows highly sensitive fluorescence detection. To reduce the separation time and preserve the unstable binding complex during injection and separation, the pre-equilibrated sample mixture was loaded near the detection window by controllable air pressure-assisted injection (Fig. 1A, left). Then the loaded sample was analysed through CE-LIF detection under running buffer (Fig. 1A, right). The selected substrates, histone peptides (pI ∼12.8) and U2 snRNA (pI ∼2.5), possess opposite charges under both the binding (pH 7.4) and separation (pH 7.5) conditions; their binding complexes were predicted to possess a negative charge. Hence the binding complexes and free U2 snRNA move toward the detection window while free peptides move toward the opposite direction through negative voltage-driven electrophoresis performed on a neutral capillary free of EOF. Peptides were fluorescently labelled to rapidly identify binding complexes from unbound peptide probes (Fig. 1B).

To eliminate the EOF which can make free peptides and binding complexes migrate toward the same direction, we modified the inner surface of the capillary with a monolayer of linear PAA. Notably, PAA modification simultaneously inhibited severe adsorption of positively charged basic peptides on the inner wall of the capillary, enhancing experimental reproducibility. In addition, the free fluorescent dye, FITC, was added to serve as the internal standard (IS) which migrated much slower than the peptide–RNA complex and therefore would not interfere with LIF detection of the binding complex.

3.2 Validation of the two-direction CE migration strategy

Given the structural similarity of FITC with ethidium bromide, the most widely used DNA intercalator (Fig. S1†), we first tested whether FITC can intercalate into double-stranded DNA (dsDNA) and generate adverse interference in the following analysis of RNA–peptide interactions. For this purpose, 20 nM 93-bp dsDNA was incubated with different concentrations of FITC and then subjected to CE-LIF analysis. As shown in Fig. 2, no apparent migration change of FITC was observed when it was pre-incubated with 93-bp dsDNA molecules, indicating that FITC would not intercalate into DNA molecules and therefore the addition of FITC as the IS would not interfere with CE-LIF analysis of peptide–RNA interactions.

Next, we tested the two-direction migration CE strategy to measure weak peptide–RNA interactions. As expected, the positively charged FITC-labelled peptide cannot migrate toward the detection window through a negative voltage-driven electrophoresis with a neutral capillary free of EOF (Fig. 3, line 3). However, when the peptide probe was pre-incubated with snRNA U2, a fluorescence signal was immediately observed (0–1.0 min) after the sample was injected and separated (Fig. 3, line 2), suggesting the formation of a negatively charged peptide–RNA complex which migrates toward

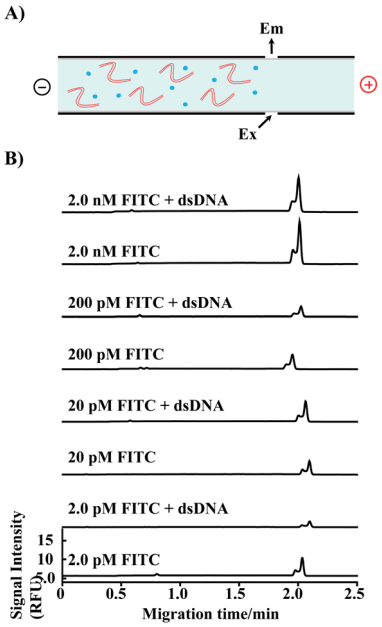

Fig. 2 No obvious migration change of FITC was observed after incubated with dsDNA. All the samples were analysed in 2× TGA running buffer.

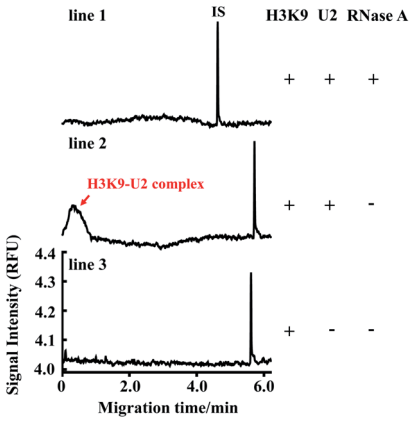

Fig. 3 Validation of two-direction affinity CE to measure weak peptide–RNA interactions. 40 nM FITC-labelled H3K9 peptide was incubated with or without 20 nM snRNA U2 at 37 °C for 30 min prior to CE-LIF analysis. For RNA digestion, 10 U RNase A was added to the pre-equilibrated sample and incubated at 37 °C for 30 min prior to CE-LIF analysis. IS: 20 pM FITC.

the detection window. To further identify this RNA-involved complex, RNase A was added to the pre-equilibrated sample to digest snRNA U2 prior to CE analysis. Indeed, the signal at 0–1.0 min completely disappeared after RNase A treatment (Fig. 3, line 1), indicating that this signal represents the peptide–RNA complex. Taken together, these results suggest that the newly proposed two-direction migration strategy is able to qualitatively detect weak and unstable peptide–RNA interactions by decreasing the migration time of the unstable complexes and regulating the free probes to move toward the opposite direction.

3.3 Application of the two-direction CE migration strategy to study peptide–RNA interactions

Having confirmed the feasibility of the two-direction CE migration strategy, we next applied it to explore potential weak interactions. In eukaryotes, histone is a class of the most vital proteins that directly pack DNA into highly ordered chromatin and play essential roles in the initiation of DNA replication, the regulation of gene expression, and the maintenance of genome stability.[39] In addition, several histone modifications can affect the structure of chromatin and regulate these fundamental processes involved in DNA.[40] Simultaneously, an increasing number of RNA molecules have been revealed to co-localize with chromatin and participate in these regulation processes.[41] For instance, snRNA U1 was recently identified to recruit long noncoding RNAs to regulatory sites of chromatin,[42] suggesting another important role of snRNA in addition to the processing of precursor messenger RNA. Herein, by using this two-direction migration affinity CE approach, we explored probable affinity interactions between snRNA U2 (Fig. S2†), another spliceosome RNA, and basic histone peptides derived from human histone H3 and H4.

Two basic peptides, H3K9 peptide and H4R3 peptide, and their corresponding methylated products, H3K9me2 peptide and H4R3me peptide (see also Section 2.3), were synthesised and labelled with FITC as fluorescent probes, respectively. Each peptide (20 nM) was incubated with varying concentrations of

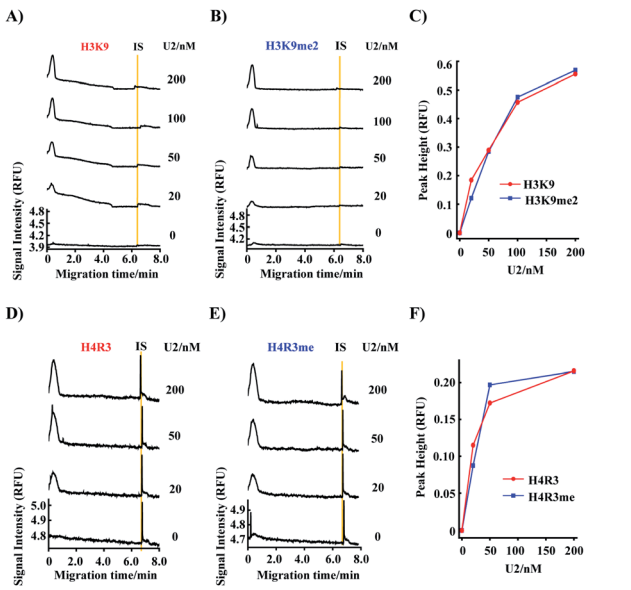

Fig. 4 Application of two-direction affinity CE to explore the affinity interactions between snRNA U2 and histone peptides. (A and B) Electropherograms obtained from CE-LIF analysis of H3K9 peptide–snRNA U2 (A) and H3K9me2 peptide–snRNA U2 (B) interactions. (C) Peak height of the detected peptide–RNA complex shown in (A) and (B). (D and E) Electropherograms obtained from CE-LIF analysis of H4R3 peptide–snRNA U2 (D) and H4R3me peptide–snRNA U2 (E) interactions. (F) Peak height of the detected peptide–RNA complex shown in (D) and (E). Each peptide (20 nM) was incubated with different concentrations of snRNA U2 (0–200 nM as indicated) at 37 °C for 30 min prior to CE-LIF analysis. IS: 20 pM FITC.

U2 snRNA (0–200 nM as indicated) and then subjected to CE-LIF analysis. As shown in Fig. 4, the peak of each peptide–RNA complex (0.3 min) conspicuously increased along with increasing concentrations of U2 snRNA whereas no significant difference was observed between unmethylated and methylated peptides, suggesting that 200 nM U2 snRNA is far from enough for saturated binding to 20 nM peptide and the methylation states have little influence on these peptide–RNA interactions.

By this method, we can observe qualitatively the weak interaction of basic peptides and RNA, but it remains a challenge to quantitatively measure the binding constant and dissociation rate. However, our method provides a new solution to the study of weak affinity and for further innovation of quantitative measurements.

4. Conclusion

In summary, we proposed and demonstrated a two-direction migration strategy that enables affinity CE to qualitatively detect weak and unstable affinity interactions by decreasing the migration distance of the binding complex and controlling the opposite migration direction of the free probe. In addition, by utilizing this two-direction migration CE approach to explore potential interactions between U2 snRNA and histone peptides, we discovered that these peptide–RNA interactions are very weak (the K_d value is estimated at the millimolar level, data not shown) and are probably caused by electrostatic attraction. Therefore the methylation states of histone peptides have little influence on their weak interactions. In the present work, two-direction migration of the binding complex and the free probe possessing opposite electric charges was achieved by eliminating the EOF. It is notable that two-direction CE migration of targets possessing identical charges can also be achieved by adjusting the mobility of the EOF, which has been theoretically and experimentally demonstrated by Le *et al.*[43] Hence, we hope that this two-direction migration CE approach will be applicable to the investigation of more probable weak and transient affinity interactions.

Conflicts of interest

There are no conflicts to declare.

Acknowledgements

This work was supported by grants from the National Research Program for Key Issues in Air Pollution Control (No. DQGG0401), the National Natural Science Foundation of China (No. 21927807, 91743201, and 21527901), the Key Research Program of Frontier Sciences, CAS (QYZDJ-SSW-DQC017), and the K. C. Wong Education Foundation.

References

1 I. J. Colton, J. D. Carbeck, J. Rao and G. M. Whitesides, *Electrophoresis*, 1998, **19**, 367–382.
2 P. Dubský, M. Dvořák and M. Ansorge, *Anal. Bioanal. Chem.*, 2016, **408**, 8623–8641.
3 M. Dvořák, J. Svobodová, M. Beneš and B. Gaš, *Electrophoresis*, 2013, **34**, 761–767.
4 F. Yu, Q. Zhao, D. Zhang, Z. Yuan and H. Wang, *Anal. Chem.*, 2019, **91**, 372–387.
5 Y. F. Cheng and N. J. Dovichi, *Science*, 1988, **242**, 562.
6 D. Zhang, M. Lu and H. Wang, *J. Am. Chem. Soc.*, 2011, **133**, 9188–9191.
7 Y.-H. Chu, Y. M. Dunayevskiy, D. P. Kirby, P. Vouros and B. L. Karger, *J. Am. Chem. Soc.*, 1996, **118**, 7827–7835.
8 C. C. Huang, Z. Cao, H. T. Chang and W. Tan, *Anal. Chem.*, 2004, **76**, 6973–6981.
9 J. N. Rauch, J. Nie, T. J. Buchholz, J. E. Gestwicki and R. T. Kennedy, *Anal. Chem.*, 2013, **85**, 9824–9831.
10 C. M. Ouimet, M. Dawod, J. Grinias, V. A. Assimon, J. Lodge, A. K. Mapp, J. E. Gestwicki and R. T. Kennedy, *Analyst*, 2018, **143**, 1805–1812.
11 C. M. Ouimet, H. Shao, J. N. Rauch, M. Dawod, B. Nordhues, C. A. Dickey, J. E. Gestwicki and R. T. Kennedy, *Anal. Chem.*, 2016, **88**, 8272–8278.
12 Y. Sun, S. Cressman, N. Fang, P. R. Cullis and D. D. Chen, *Anal. Chem.*, 2008, **80**, 3105–3111.
13 S. Štěpánová and V. Kašička, *J. Sep. Sci.*, 2015, **38**, 2708–2721.
14 M. Gong, K. R. Wehmeyer, P. A. Limbach and W. R. Heineman, *Electrophoresis*, 2007, **28**, 837–842.
15 B. Zhao, D. Zhang, C. Li, Z. Yuan, F. Yu, S. Zhong, G. Jiang, Y. G. Yang, X. C. Le, M. Weinfeld, P. Zhu and H. Wang, *Cell Discovery*, 2017, **3**, 16053.
16 A. Taga, R. Satoh, S. Ishiwata, S. Kodama, A. Sato, K. Suzuki and R. Sugiura, *J. Pharm. Biomed. Anal.*, 2010, **53**, 1332–1337.
17 D. Zou, D. Zhang, S. Liu, B. Zhao and H. Wang, *Anal. Chem.*, 2014, **86**, 1775–1782.
18 H. Wang, M. Lu and X. C. Le, *Anal. Chem.*, 2005, **77**, 4985–4990.
19 J. Wang, Z. Zhu, L. Qiu, J. Wang, X. Wang, Q. Xiao, J. Xia, L. Liu, X. Liu, W. Feng, J. Wang, P. Miao and L. Gao, *Nanotechnology*, 2018, **29**, 274001.
20 E. Farcaș, J. Hanson, L. Pochet and M. Fillet, *Anal. Chim. Acta*, 2018, **1034**, 214–222.
21 V. Šolínová, L. Žáková, J. Jiráček and V. Kašička, *Anal. Chim. Acta*, 2019, **1052**, 170–178.
22 C. Artner, H. U. Holtkamp, W. Kandioller, C. G. Hartinger, S. M. Meier-Menches and B. K. Keppler, *Chem. Commun.*, 2017, **53**, 8002–8005.
23 M. Girardot, P. Gareil and A. Varenne, *Electrophoresis*, 2010, **31**, 546–555.
24 V. Šolínová, H. Mikysková, M. M. Kaiser, Z. Janeba, A. Holý and V. Kašička, *Electrophoresis*, 2016, **37**, 239–247.
25 H. Wang, M. Lu, M.-s. Tang, B. Van Houten, J. B. A. Ross, M. Weinfeld and X. C. Le, *Proc. Natl. Acad. Sci. U. S. A.*, 2009, **106**, 12849.
26 F. Yu, Z. Yuan, D. Zhang, Y. Liu, Q. Zhao and H. Wang, *Chem. Commun.*, 2020, **56**, 7402–7406.
27 A. M. Baig, A. Khaleeq, U. Ali and H. Syeda, *ACS Chem. Neurosci.*, 2020, **11**, 995–998.

28 A. Staub, S. Comte, S. Rudaz, J. L. Veuthey and J. Schappler, *Electrophoresis*, 2010, **31**, 3326–3333.
29 P. F. Dillon, *Biophysics: A Physiological Approach*, Cambridge University Press, Cambridge, 2012.
30 H. Wang, M. Lu, M. Weinfeld and X. C. Le, *Anal. Chem.*, 2003, **75**, 247–254.
31 H. Wang, M. Lu and X. C. Le, *Anal. Chem.*, 2005, **77**, 4985–4990.
32 C. M. Ouimet, H. Shao, J. N. Rauch, M. Dawod, B. Nordhues, C. A. Dickey, J. E. Gestwicki and R. T. Kennedy, *Anal. Chem.*, 2016, **88**, 8272–8278.
33 M. Kanoatov, V. A. Galievsky, S. M. Krylova, L. T. Cherney, H. K. Jankowski and S. N. Krylov, *Anal. Chem.*, 2015, **87**, 3099–3106.
34 S. Hjertén, *J. Chromatogr. A*, 1985, **347**, 191–198.
35 J. Bodnar, L. Hajba and A. Guttman, *Electrophoresis*, 2016, **37**, 3154–3159.
36 G. E. Zentner and S. Henikoff, *Nat. Struct. Mol. Biol.*, 2013, **20**, 259–266.
37 C. Jiang and B. F. Pugh, *Nat. Rev. Genet.*, 2009, **10**, 161–172.
38 Z. Q. Pan and C. Prives, *Genes Dev.*, 1989, **3**, 1887–1898.
39 J. V. Chodaparambil, R. S. Edayathumangalam, Y. Bao, Y. J. Park and K. Luger, *Ernst Schering Res. Found. Workshop*, 2006, pp. 29–46.
40 A. J. Bannister and T. Kouzarides, *Cell Res.*, 2011, **21**, 381–395.
41 M. Magistri, M. A. Faghihi, G. St Laurent III and C. Wahlestedt, *Trends Genet.*, 2012, **28**, 389–396.
42 S. Shinkai, T. Nozaki, K. Maeshima and Y. Togashi, *PLoS Comput. Biol.*, 2016, **12**, e1005136.
43 A. T. H. Le, S. M. Krylova, M. Kanoatov, S. Desai and S. N. Krylov, *Angew. Chem., Int. Ed.*, 2019, **58**, 2739–2743.

